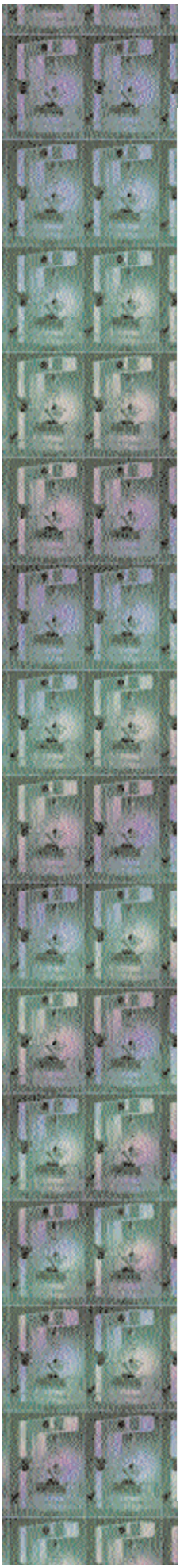

Amplifying quantum signals with the single-electron transistor

Michel H. Devoret*† & Robert J. Schoelkopf*

**Department of Applied Physics, Yale University, New Haven, Connecticut 06520, USA*
†Service de Physique de l'Etat Condensé, CEA-Saclay, F-91191, France

Transistors have continuously reduced in size and increased in switching speed since their invention in 1947. The exponential pace of transistor evolution has led to a revolution in information acquisition, processing and communication technologies. And reigning over most digital applications is a single device structure — the field-effect transistor (FET). But as device dimensions approach the nanometre scale, quantum effects become increasingly important for device operation, and conceptually new transistor structures may need to be adopted. A notable example of such a structure is the single-electron transistor, or SET[1–4]. Although it is unlikely that SETs will replace FETs in conventional electronics, they should prove useful in ultra-low-noise analog applications. Moreover, because it is not affected by the same technological limitations as the FET, the SET can approach closely the quantum limit of sensitivity. It might also be a useful read-out device for a solid-state quantum computer.

It is now possible to put a billion transistors on a single chip operating with a clock period of a billionth of a second. Most probably, the trend in reducing dimensions and times will continue in the next decade. But as the number and density of gates and memory elements increase, the energy of signals also has to be reduced to keep the power dissipation sufficiently low.

Surprisingly, even though the size of a typical transistor in a microcomputer chip is now just a few hundred nanometers, its functioning remains essentially classical: quantum mechanics only enters in the explanation of the values of the physical parameters of materials, like the band-gap of a semiconductor. Otherwise, the discreetness of matter and the wave-like properties of electrons can be largely ignored in the understanding of the behaviour of electrical signals in today's integrated circuits.

But as devices get smaller, faster and more densely packed, quantum effects will have increasingly to be taken into account. Even well before we reach the ultimate limit where transistors are reduced to the size of an atom or a molecule, we encounter four limits. Quantum phenomena become significant when (1) signal energy, (2) signal charge, (3) device dimension, and (4) device size tolerance approach, respectively, the energy of one photon, the charge of one electron, the electron wavelength, and the size of one atom.

Much research has been devoted to assess if quantum effects arising from these conditions will force the adoption of new physical principles or if they can simply be tamed by better control of the chip structure at the atomic level. To our knowledge, there is no general consensus on the answer to this question.

Another research direction has been to exploit quantum effects arising in devices of nanometer scale to implement a function that cannot be performed by present devices. In some applications, which operate at limits (1) or (2) or both, it is not only inevitable but also desirable. In astronomy, for instance, it is important to extract as much information as possible from a single photon[5]. Recent advances in quantum information theory[6] indicate that scalable switching elements that behave fully as quantum systems would not simply make calculations with minimal energy, they could in addition perform tasks that would be impossible with conventional computers. In a quantum computer, usual bits are replaced by quantum bits or 'qubits' which can be 'entangled' with each other, thereby carrying a new type of information that is useful in solving highly parallel tasks. New types of devices are needed to read-out such qubits, that is, to amplify their associated single-quantum signals.

In the realm of atomic physics and quantum optics, the detection of individual microscopic particles travelling in vacuum, such as photons and electrons, is now performed routinely with almost unity efficiency by instruments derived from the photomultiplier. However, the measurement of electrical signals resulting from the motion of a single electron in a circuit involves an amplifier having not only a good energy sensitivity, but also electrical characteristics that are adapted to this circuit.

A particularly simple and spectacular example of such a device is the single-electron transistor (SET)[1–3], which exploits the quantum phenomenon of tunnelling to control and measure the movement of single electrons inside a solid-state circuit. SETs are extremely precise solid-state electrometers[4,7], already out-performing state-of-the-art conventional transistors[8] by three orders of magnitude. Their charge sensitivity has been shown to be as low as a few $10^{-5}\,e/\sqrt{\mathrm{Hz}}$, which means that a charge variation of $10^{-5}\,e$ can be detected in a measurement time of 1 s (the precision improves as the square root of the measurement time). This result is only an order of magnitude away from the theoretical limit of $10^{-6}\,e/\sqrt{\mathrm{Hz}}$. SETs have applications in metrology[9] and single-photon detection[10,11]. Furthermore, it has been realized in the past few years that SETs can perform a measurement on a single quantum two-state system (qubit)[12,13], perturbing its quantum evolution in a minimal way. That is, the SET is a charge amplifier operating in the vicinity of the quantum limit. It would be a practical read-out device for several solid-state implementations of qubits[14]. In this article we review these latest developments.

Conventional transistors

Before discussing the performance of SETs, it is useful to recall the operating principle of the most common transistor,

the metal-oxide semiconductor field-effect transistor (MOSFET). Figure 1 depicts schematically the layout of the device and its operating principle (we restrict ourselves here to the nMOSFET, in which the majority charge carriers are electrons). Two conducting electrodes, called the source and drain, are connected by a channel made of a material in which the number of conduction electrons can be varied, in practice a semiconductor (Fig. 1a). A voltage is applied to the 'gate', a third conducting electrode that is separated from the channel by a thin insulating layer. When the gate–source voltage is zero, there are no conduction electrons in the channel as the effective potential they would experience there is larger than in the leads (Fig. 1b). The channel is therefore in an insulating state. But when the gate voltage is increased with respect to the source, the potential experienced by the electrons in the channel decreases and they populate the channel just under the gate (Fig. 1c). The channel becomes conducting. The larger the gate voltage, the larger will be the channel electron population that can participate in the current. Eventually, all the electron states in the energy window set by the source–drain voltage can propagate through the channel and the current no longer depends on the gate voltage. This saturation regime is depicted in Fig. 1d.

This field effect provides an amplification mechanism since an increase in gate voltage, bringing a modest current to the gate electrode, can switch on a larger current through the channel (Fig. 2). The source–drain current is determined by the conductance of the channel, which in turn depends on two factors: the density of its conduction electrons and their mobility. The electron density is controlled directly by the gate voltage. The electron mobility is set by the collisions of electrons with static irregularities of the crystal as well as with its dynamic deformations due to thermal agitation. When thermal agitation is the predominant factor, electron mobility is, to a large extent, independent of the gate voltage. However, at low temperatures, mobility can also increase when the density increases, reinforcing the influence of the gate voltage on the source–drain current.

Note that so far we have made no reference to the wave-like properties of electrons nor to the fact that the channel is made from individual atoms. The only quantum property that has had a role in our explanation is the Pauli principle, which dictates that each possible state for an electron in the channel can be occupied at most by only one electron. This means that only a certain number of electrons can accumulate in the channel, setting a limit on the current flow.

However, the quantum properties of electrons and atoms will be increasingly important as FETs are made smaller. For example, the wave nature of electrons will influence the way they travel through the channel. When the transverse dimension of the channel becomes comparable to the wavelength of electrons (around 100 nm), electron propagation becomes more sensitive to the atomic disorder in the device, which is inherent in the present fabrication process. The disorder makes the channel remain insulating even when the density of electrons is increased. Effects of this kind, which result from reaching the limit to device dimension (limit (3) above), pose a major problem if the reduction of size is not accompanied by an improvement in the atomic structure of the fabricated devices.

If, however, the atomic structure of the FET could be made defect-free, a recent analysis[15] shows it would continue to function in the regime where the electron propagation in the channel is wave-like. It would thus 'break' limit (3) and could be further scaled down until a channel length of about 8 nm is reached, a stage at which limit (4) seems to severely affect the performance of the FET.

In an ideal situation, we might want electrons to be scattered only by the gate-dependent potential, with other scattering mechanisms always being detrimental to amplification. But the confinement of electrons in the channel by tunnel barriers, in the source–drain direction, can also lead to a new kind of amplification principle. This is the basis of the SET. As we shall see, this new principle circumvents the problem of the FET that the gate capacitance, which is an important factor in determining charge sensitivity, is tied to the size of the channel. Until the technology for reliably fabricating FETs with channels of nanometre-scale dimensions has been developed, the SET is the best device in terms of charge sensitivity.

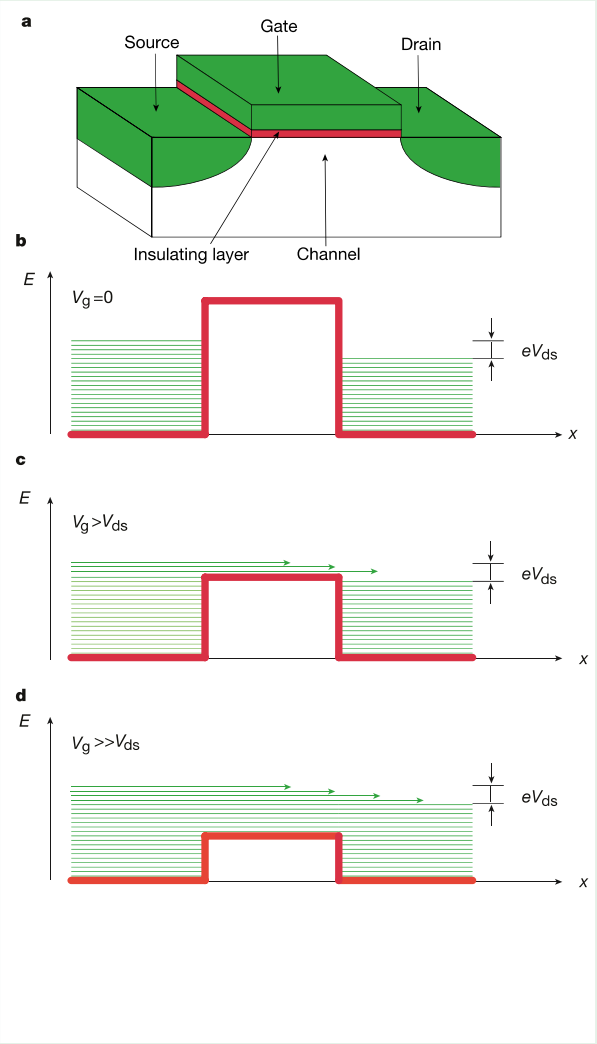

Figure 1 Principle of a metal-oxide semiconductor field-effect transistor (MOSFET). **a**, The device consists of two conducting electrodes (source and drain) connected by a semiconducting channel. The channel is influenced electrostatically by the gate, a conducting electrode separated from the channel by thin insulating layer. **b**, When the voltage applied between the gate and the source is zero, the Fermi energy of the source and drain lies in the gap of the semiconductor. Here, we sketch the potential (red curve) seen by conduction electrons when they travel from source to drain along a line in the channel just under the gate. There are no filled electron states (green lines) in the channel, which as a result remains insulating. **c**, When the gate voltage is increased, the potential seen by conduction electrons is lowered. There are now filled states in the channel at the Fermi energy of the source and drain. The device conducts. **d**, When the gate voltage is increased further, the current finally saturates when all the states in the bias window are filled.

Operating principle of SETs

Unlike the FET, whose principle does not require the motion of electrons to be quantum-mechanical, the SET is based on an intrinsically quantum phenomenon: the tunnel effect through a metal–insulator–metal junction. When two metallic electrodes are separated by an insulating barrier whose thickness is only ~1 nm, electrons at the Fermi energy can traverse the insulator even though their energy is too

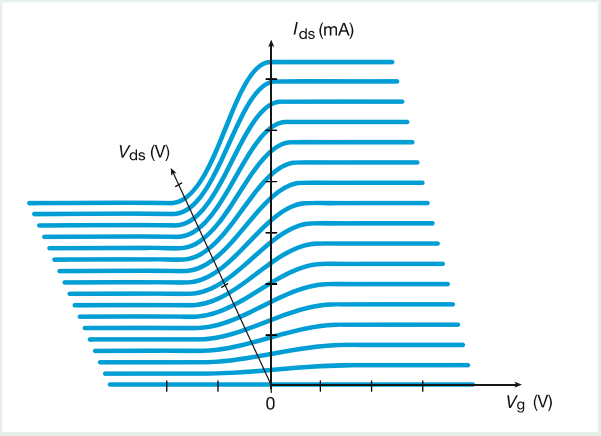

Figure 2 Variation of the source–drain current in a MOSFET as a function of the gate voltage. When the gate voltage is increased from zero, the source–drain current is turned on. This device can be used both in digital electronics and as an amplifier for analog signals.

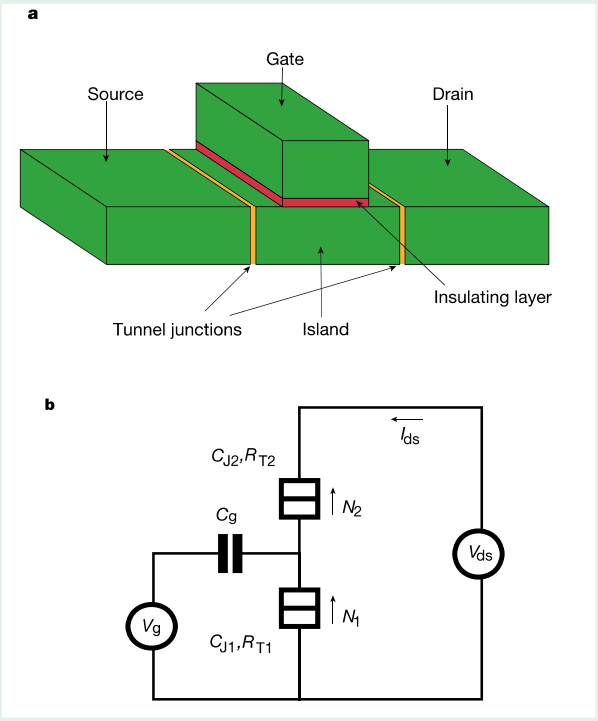

Figure 3 The single-electron tunnelling transistor (SET). **a**, Simplified three-dimensional structure of the SET. The channel of the FET is replaced here by a sandwich consisting of a nanoscale metal electrode (island), which is connected to the drain and the source by tunnel junctions. As in the FET, a gate electrode influences the island electrostatically. **b**, Circuit diagram of the SET. The square box symbol represents a tunnel junction, and integers N_1 and N_2 denote the numbers of electrons having tunnelled through the two junctions. Each junction is characterized by its capacitance and its tunnel resistance.

low to overcome, in a classical motion, the large potential barrier of the insulating region. The tunnel effect manifests itself by a finite resistance R_T of the insulating barrier. This resistance depends both on the transmission coefficient $\mathcal{T}$ of the barrier to electron waves (which is an exponentially decreasing function of its thickness) and on the number M of independent electron wave modes impinging on the barrier (this number is equal to the area of the junction divided by the square of the electron wavelength). The SET uses a key property of the tunnel effect in a many-electron system: for barriers such that $\mathcal{T}M \ll 1$, the charge Q transferred through the barrier becomes quantized with $Q = Ne$, where N is an integer[16]. In other words, for N not to be subject to quantum fluctuations, the resistance of the junction must be large compared with the resistance quantum $R_T \gg h/e^2 = R_K = 25.8\,\mathrm{k\Omega}$ (refs 17,18).

The SET consists of two such tunnel junctions placed in series (Fig. 3a,b). An 'island' is thus formed between the two junctions. A gate electrode is coupled electrostatically to the island. The SET can thus be described as a FET in which the semiconducting channel has been replaced by a metallic island sandwiched between two tunnel barriers. The island has a total capacitance C_Σ, which the sum of the gate and junction capacitances $C_\Sigma = C_g + C_{J1} + C_{J2}$.

If the dimensions of the island are sufficiently small, the charging energy $E_C = e^2/(2C_\Sigma)$ of one extra electron in the island will become larger than the energy of thermal fluctuations: $E_C \gg k_B T$, where k_B is the Boltzmann constant and T is temperature. In practice, for devices fabricated by standard electron-beam lithography, C_Σ is of the order of a femtofarad and the charging energy is of order 1 K, necessitating temperatures below 300 mK to satisfy the above charging energy criterion. Over the past few years, however, experiments have shown that with advanced fabrication methods, room temperature operation is possible[19–21].

Because electrons interact strongly via the Coulomb interaction when they pass through the island, the analysis of the SET differs fundamentally from that of the FET. In the FET, electrons go from source to drain independently, and in such numbers that one can consider that the potential seen by one is an average which does not depend on the configuration adopted by all of the others. Electrical transport results from a simple addition of the motion of each electron. In the SET, by contrast, transport results from transitions between collective charge states of the system. These charge states are described by the two numbers N_1 and N_2 of electrons having traversed the junctions (Fig. 3b).

The behaviour of the device is governed by the global electrostatic energy[16] $E_{el} = E_C[N_2 - N_1 - (C_g V_g/e) - (C_2 V_{ds}/e) + q_0]^2 - eN_2 V_{ds}$, which includes the energy stored in the junction and gate capacitances, as well as the work done by the voltage sources. Here, V_g and V_{ds} are the voltages applied between gate and source, and drain and source, respectively. The so-called offset gate charge q_0 is a phenomenological quantity describing the fact that electric fields in the capacitances of the system are non-zero even when the island is neutral and when no voltage is applied. It takes a randomly different, non-integer value for each device and cool-down. It also fluctuates slowly in time with a $1/f$ spectral density[22]. We will discuss its effect in more detail below. But as far as the amplification mechanism of the SET is concerned, we can treat it as a constant.

According to the so-called 'global rules', also known as 'orthodox theory', tunnel events will take place independently on each junction at a rate governed by the global energy, provided that the junction resistances satisfy $R_{T1}, R_{T2} \gg R_K$ and that the voltage sources V_g and V_{ds} have negligible internal impedance, on the scale of the resistance quantum, around the Coulomb frequency $E_C/\hbar$ (ref. 17).

In this regime, each tunnel event creates one electron–hole pair, the electron and the hole being on opposite sides of the junction. The succession of tunnel events constitutes a Poisson process. More specifically, a tunnel event will take place on junction i with a rate given by $\Gamma_i = [1/(R_{Ti}e^2)][\Delta E_i/(1 - \exp(-\Delta E_i/k_B T))]$ where $\Delta E_i = E_{el}\{N_i^{before}, N_j\} - E_{el}\{N_i^{after}, N_j\}$.

At zero temperature, tunnel events take place only if they are energetically allowed, that is, $\Delta E_i > 0$. For a drain–source voltage below the Coulomb gap voltage e/C_Σ, the current therefore depends critically on the value of the gate voltage. If the gate voltage is such that

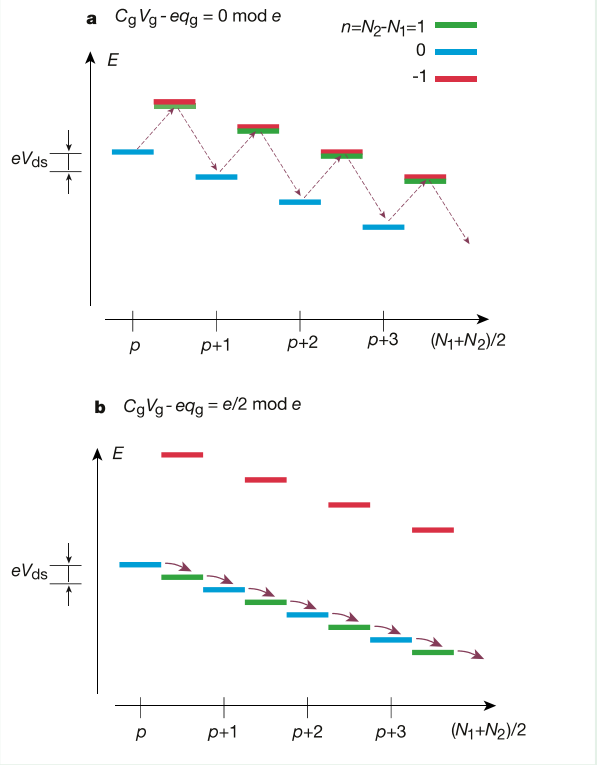

Figure 4 Charge levels of the SET. **a**, Charge levels in the full Coulomb blockade; **b**, charge levels in the lifted Coulomb blockade case. The integers N_1 and N_2 denote the numbers of electrons having tunnelled through the two junctions (see Fig. 3). In **a**, the only possible conduction process is co-tunnelling, that is, a weak second-order process involving the tunnelling of two electrons on two different junctions and a virtual charge state (dashed purple arrows). In **b**, the main conduction process is a cascade of tunnel events involving the two junctions sequentially (full purple arrows).

$C_gV_g = q_0e$ mod e, the island has a well defined number of electrons. Tunnel events cannot take place on the junctions because the global energy would increase (Fig. 4a) and the current is zero. This is the phenomenon of Coulomb blockade. But if the gate voltage is such that there is a charge equivalent to one half electron on the gate capacitance, $C_gV_g = (q_0 + \frac{1}{2})e$ mod e, tunnel events are energetically allowed (Fig. 4b). A cascade of transitions between charge states occurs, and current flows between source and drain.

Note that in practice the current cannot be turned off completely in the Coulomb-blockaded state. Higher-order processes in which several tunnel events occur simultaneously (co-tunnelling processes), and whose relative importance scale as powers of R_K/R_T, will induce a small leakage current not described by the orthodox theory. However, as long as $R_K \gg R_T$, the SET behaves as a charge amplifier as the presence or absence of a fraction of an electron on the gate capacitance can control an easily measurable current (the order of magnitude is around 10^9 e/s in practical cases) (Fig. 5). This gain is not the only factor determining the sensitivity of the device. One must take into account the shot noise in the source–drain current, which is attributable to the quantum randomness of the time intervals between tunnel events (we work in a regime where thermal fluctuations can be neglected). This quantum randomness, corresponding to electrons having to 'choose' between the two sides of the barrier, is the process that ultimately limits the sensitivity of the device. As we will show below, the noise characteristics of the SET can be calculated exactly in a simple regime, which is rich enough to yield semi-quantitative understanding of the quantum limit of sensitivity.

Returning to the offset gate charge, it is believed that its value is determined in part by differences between the work functions of the metal of the island and that of the other electrodes. Even minute variations in the work functions are sufficient to cause q_0 to fluctuate by numbers much greater than unity, which is the case observed in practice. Another potential source of fluctuation in offset charge is charge motion in the substrate or even in the tunnel barrier oxide. The absence of control over offset charges severely hinders any application of SETs to digital electronics, where the gate thresholds must be rigorously fixed and uniform. However, SETs can still be used as sensitive amplifiers in the audio-frequency (a.f.) or radio-frequency (r.f.) domains, as a simple additional feedback circuit can compensate for the fluctuations in offset charge that occur mainly at lower frequencies.

Noise characteristics of an amplifier

Before we examine how quantum shot noise affects the ultimate performances of SETs, it is useful to discuss the noise properties of a general amplifier.

A linear amplifier can be described phenomenologically as a 'black box' with two input leads and two output leads. We can represent the inside of the black box by effective elementary components which accurately describe how it appears to the outside circuitry. If we limit ourselves to the simpler case where the amplifier has no feedback (that is, input current is independent of output voltage), we arrive at the schematics of Fig. 6 (feedback introduces complications that are not crucial in our discussion). Three elements describe the transformation of the signal by the amplifier: an ideal voltage amplifier with infinite input impedance, zero output impedance and a voltage gain $G(\omega)$, and the input and output impedances, $Z_{in}(\omega)$ and $Z_{out}(\omega)$. In these parameters, the argument ω denotes the signal angular frequency.

In addition, the random fluctuations due to the amplifier are described by two noise sources with very different roles. The voltage noise source V_N describes the output noise, that is, the noise added by the amplifier to the output signal, referred to the input. The current noise I_N, on the other hand, describes the back-action of the amplifier on the circuit at the input. The voltage and current noise are assumed to be gaussian, and are characterized by the spectral densities $S_V(\omega)$ and $S_I(\omega)$, which are the Fourier transforms of the autocorrelation functions of V_N and I_N, respectively. We neglect here the correlations $S_{VI}(\omega)$, which are not essential for our discussion. These spectral densities, together with the input impedance, determine the ultimate resolving power of the amplifier for small signals.

It is useful, in the discussions of this resolving power, to introduce several combinations of these quantities. The first one is the charge sensitivity $\delta Q(\omega) = \sqrt{S_V(\omega)}/|\omega Z_{in}(\omega)|$, which we have already discussed. The second quantity is the energy sensitivity $\epsilon(\omega) = \delta Q^2(\omega)/2C_{in}$ where $C_{in} = \mathrm{Re}\{1/[i\omega Z_{in}(\omega)]\}$. Assuming that the amplifier is driven by a voltage source with strictly zero internal impedance (and hence always in the classical regime, as the zero-point voltage fluctuations are proportional to the real part of the impedance), this quantity tells us the smallest amount of energy $\delta E = \epsilon/\tau$ fed by the source into the input circuit of the amplifier which will give an output signal that is distinguishable from zero when we accumulate it during a time τ. Even though ϵ has the dimension of an action and is conveniently measured in units of $\hbar$, quantum mechanics does not impose any restriction on the ratio $\epsilon/\hbar$, which can in principle tend to zero[23]. Nevertheless, in systems studied so far, a value of $\epsilon/\hbar$ of order unity usually means that the contribution of thermal fluctuations to the noise of the amplifier have been suppressed down below those of quantum fluctuations.

Although the energy sensitivity seems initially to be a very powerful concept, it neglects the back-action of the amplifier and is insufficient to determine how well the amplifier performs when we use it to measure a quantum signal coming from a system with a finite source impedance Z_S. The current noise, which induces back-action voltage fluctuations across the source impedance, and hence on the

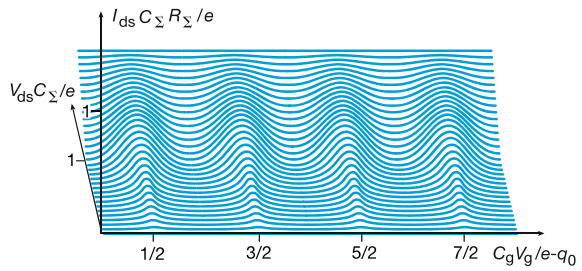

Figure 5 Variation at $T = 0$ of the source–drain current in a SET as a function of the voltage between drain and source and the voltage between gate and source. We have assumed that the two junctions have identical parameters. The sum of the junction tunnel resistances R_Σ is twice the resistance quantum h/e^2 and a small amount of co-tunnelling rounds the peaks associated with the lifting of the Coulomb blockade (gate charge corresponding to half-integers multiplied by the charge quantum). The sensitivity of the SET is based on the rapid variation of the source–drain current as the gate charge varies by a fraction of one electron.

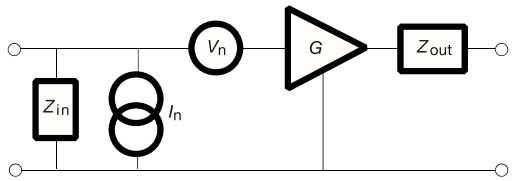

Figure 6 Effective circuit elements describing the properties of a linear voltage amplifier with no feedback. The triangle represents an ideal noiseless voltage amplifier with infinite input impedance and zero output impedance. Its gain is denoted by G. The boxes marked Z_{in} and Z_{out} correspond to the input and output impedances, respectively. The noise sources V_N and I_N represent the voltage noise (noise added by the amplifier at the output, but referred to the input) and the current noise (back-action noise of the amplifier sent to the circuit feeding the input). These elements are eventually dependent on the signal frequency ω

signal going into the amplifier, must be considered together with the voltage noise.

We therefore introduce the noise impedance $Z_N = \sqrt{S_V/S_I}$ and the noise energy $E_N = \sqrt{S_V S_I}$. They have the following meaning: supposing that $1/Z_{in}(\omega) = 0$, the amplifier will add a minimal amount of noise to the signal coming from the source when $Z_S = Z_N$ (noise matching). This minimal noise has a power per unit bandwidth given by E_N (this quantity has the dimension of an energy, hence the name noise energy). Quantum mechanics places a strict restriction on the noise energy. No amplifier can have an E_N smaller than $\hbar\omega/2$, half a photon energy at the signal frequency ω (refs 23–25). This fundamental limitation is a form of Heisenberg's uncertainty principle (see Table 1). It is worth mentioning that in the classical regime, that is, the regime where the contribution of quantum fluctuations to the noise of the amplifier is negligible, the noise temperature $T_N = E_N/k_B$ is often used in place of the noise energy. The meaning of T_N corresponds to a well-defined procedure: imagine one connects a resistor with value Z_N at the input of the amplifier. The temperature to which one must heat the resistor to double the noise measured at the output of the amplifier is precisely T_N.

If we now apply these concepts to FET amplifiers, we find that the best performance in the r.f. domain 0.1–10 GHz is obtained with heterostructure FETs cooled to 4 K (ref. 26). At 500 MHz, their noise temperature is around 2 K (the corresponding thermal energy is equivalent to the energy of 40 photons at 1 GHz), their noise impedance is about 50 Ω and their energy sensitivity is of the order $10^2\,\hbar$. They are thus far from the quantum limit (at higher frequencies the minimum noise energy improves and can be equivalent to only ten photons). As a charge-sensing device, their best performance is around $10^{-2}\,e/\sqrt{\text{Hz}}$ (ref. 8).

Although theoretically the heterostructure FET could reach the quantum limit of sensitivity in the form of a ballistic, two-dimensional electron gas quantum-point contact[27], it is difficult in this device to achieve effective electrostatic coupling of the gate electrode to the channel without affecting its mobility and inducing parasitic input capacitance. In the SET, by contrast, there is more flexibility in the design of the gate capacitance. The fabrication of the latter is to a large extent disconnected from that of the tunnel barriers, whose quality is analogous to the mobility of the channel in the FET. We will now examine how the operating principle of the SET brings us close to the quantum limit.

Ultimate sensitivity of SETs

In the framework of the orthodox theory, the tunnel events constitute a generalized Poisson process with correlations. It is possible to calculate analytically the noise characteristics of the SET at temperatures such that $k_BT \ll eV_{ds}$ (refs 7, 28). The following expressions are obtained for the voltage and current noise, in the simple case where the two junctions have identical parameters:

$$S_V(\omega) = \frac{(1-\alpha^2)(1+\alpha^2)}{8\alpha^2} eV_{ds}R_\Sigma\left(\frac{C_\Sigma}{C_g}\right)^2$$

$$S_I(\omega) = \frac{(1-\alpha^2)}{4}\frac{eV_{ds}}{R_\Sigma}\left(\frac{C_g}{C_\Sigma}\right)^2\left(\frac{e\omega R_\Sigma}{V_{ds}}\right)^2$$

In what follows, we neglect the influence of the correlation

$$S_{VI}(\omega) = \frac{(1-\alpha^2)}{8} eV_{ds}\left(\frac{i\omega eR_\Sigma}{V_{ds}}\right)$$

between voltage and current noise, whose effect would be to reduce the noise energy if an appropriate complex source impedance could be presented to the SET.

In these noise expressions the Coulomb blockade parameter $\alpha = (2C_gV_g - e)/C_\Sigma V_{ds}$, which is limited here to the range $0 < \alpha < 1 - \text{Max}(R_K/\pi R_\Sigma, eV_{ds}/k_BT)$, fixes the relative values of the gate and

Table 1 Constraints on sensitivity and back-action imposed by quantum mechanics

System	Sensitivity	Back-action	Limiting relation	Limited quantity
Heisenberg microscope	Δx	Δp	$\Delta x\Delta p \geq \hbar/2$	Action
Electronic amplifier	S_V	S_I	$(S_VS_I)^{1/2} \geq \hbar\omega/2$	Noise energy
Qubit read-out	T_m	Γ_ϕ	$T_m\Gamma_\phi \geq 1/2$	Information

Table 1 shows different forms of Heisenberg's uncertainty relation linking the sensitivity of a measurement of a given physical quantity and the simultaneous back-action on the conjugate quantity. The precision with which the position of an object would be measured with a photon is related to the momentum transferred to this object by the radiation pressure of the photon (row 1). Similarly, the voltage sensitivity with which an amplifier measures the circuit at its input is related to the back-action current noise that this amplifier produces in the circuit (row 2). Finally, the time needed to acquire the value of a qubit is related to the rate of dephasing of the qubit induced by the back-action of the read-out (row 3). Quantities characterizing sensitivity and back-action, respectively, are given in columns 2 and 4.

drain–source voltage. For $1 - R_K/(\pi R_\Sigma) < \alpha$, co-tunnelling processes dominate over the single tunnelling processes we consider here, and for $1 - eV_{ds}/k_BT < \alpha$ the influence of thermal fluctuations would to have be taken into account in the above expressions. The resistance $R_\Sigma = R_{T1} + R_{T2}$ is the sum of the two junction resistances. The above expressions are valid for source–drain voltages below the Coulomb gap $V_{ds}C_\Sigma/e < 1$ and at frequencies ω that are low on the tunnel rate scale $(eR_\Sigma/V_{ds})^{-1}$. We have taken the mean offset charge to be zero because it appears only as a shift in V_g, but the typical value of the expected $1/f$ offset charge fluctuations make our expressions valid only above the crossover to the intrinsic device shot noise at a few 10^5 Hz. Note that at this level of approximation the input impedance is simply a capacitance resulting from the series combination of the gate and the sum $C_J = C_{J1} + C_{J2}$ of the two junction capacitances: $Z_{in} = C_\Sigma/[i\omega C_g(C_{J1} + C_{J2})]$. A dissipative part in the input impedance appears only at higher orders in the dimensionless signal frequency $(e\omega R_\Sigma/V_{ds})^{-1}$.

It is straightforward to go from these expressions to the charge sensitivity, energy sensitivity, noise energy and noise impedance:

$$\delta Q(\omega) = \frac{C_J}{\alpha}\sqrt{\frac{(1-\alpha^4)}{8}\left(\frac{R_\Sigma}{R_K}\right)\left(\frac{hV_{ds}}{e}\right)}$$

$$\epsilon(\omega) = \frac{\pi\hbar(1-\alpha^4)}{8\alpha^2}\left(\frac{R_\Sigma}{R_K}\right)\left(\frac{V_{ds}}{e/C_\Sigma}\right)\left(\frac{C_J}{C_g}\right)$$

$$E_N(\omega) = \frac{\pi(1-\alpha^2)}{2\alpha}\sqrt{\frac{(1+\alpha^2)}{2}}\,\frac{R_\Sigma}{R_K}\hbar\omega$$

$$Z_N(\omega) = \sqrt{\frac{1+\alpha^2}{8\alpha^2}}\left(\frac{C_\Sigma}{C_g}\right)^2\frac{V_{ds}}{e\omega}$$

We can find a conservative upper bound for the optimal value of the quantities that characterize the sensitivity of the SET by minimizing the above expressions over the range of parameter values that correspond to our hypotheses. We therefore take $\alpha = 1 - 2R_K/3R_\Sigma$ and $R_\Sigma = 2R_K$, values at which co-tunnelling remains marginal. We also take the source–drain voltage $V_{ds} = e/(2C_\Sigma)$ to be able to neglect thermal fluctuations in practical situations. In addition, we take $C_J = 1$ fF as a compromise between reaching attainable temperatures, keeping the heating of the island by the drain–source current at a reasonable level and achieving an acceptable output signal (in contrast with the previous parameter choices, this last value is dictated essentially by the current technology issues and not by the validity of our expressions). We arrive at the optimal values

$$\delta Q_{opt} \lesssim 1.7\times10^{-6}\, e/\sqrt{\text{Hz}}$$
$$\epsilon_{opt} \lesssim 0.7\hbar(C_J/C_g)$$
$$E_{N\,opt} \lesssim 2.2\hbar\omega$$
$$[G\times E_N]_{opt} = 0.14eV_{ds} \lesssim 75\,\text{mK}\times k_B$$

We have left the internal coupling ratio (C_J/C_g) of the SET in the right-hand side of the expression for ϵ_{opt} as this parameter can easily be modified by changing the lithography of the device. This ratio determines how much of the energy fed by the gate voltage into the SET is used to charge the island, which is the active element, rather than the gate capacitance.

The value for $E_{N\,opt}$ shows that the SET operates in the vicinity of the quantum limit. The product $[G\times E_N]_{opt}$ gives the SET output noise which would ideally be higher than the added noise of the following amplifier, that is, a cryogenic heterostructure FET. Today, this FET is the limiting factor in the system noise, and the best experimental upper bound so far for the energy sensitivity is $\epsilon \lesssim 40\hbar(C_J/C_g)$

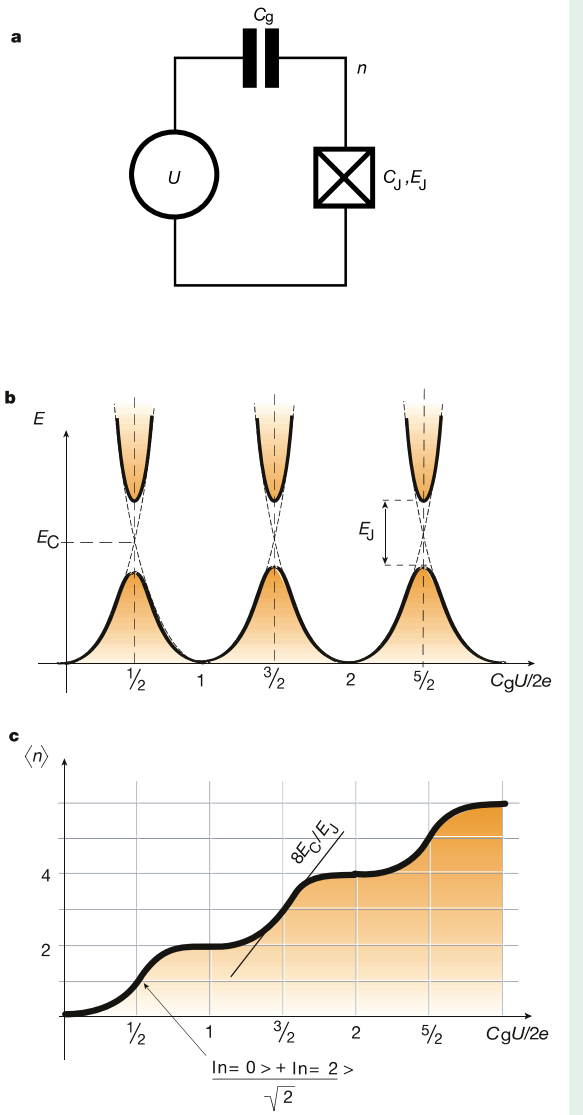

Figure 7 The single-Cooper-pair box. **a**, Circuit diagram of the single-Cooper-pair box. This simple system consists of one superconducting tunnel junction (box with cross) in series with a voltage source U and a gate capacitance C_g. When the charging energy of the island is less than the superconducting gap, all electrons are paired and the number n of excess electrons is even. Cooper pairs can tunnel reversibly through the tunnel junction. Charge states differing by one Cooper pair are coupled by the Josephson energy E_J. **b**, Energy of the two lower quantum states of the Cooper-pair box (full line) as a function of U. The dashed lines represent the electrostatic energy of the box including the work done by the voltage source. At the avoided crossings, the two charge states are mixed and constitute a solid-state implementation of a qubit. **c**, Quantum mechanical average of the number of electrons in the ground state of the box, as a function of U.

in the r.f. domain[4]. The improvement of the combination of the SET with a FET, or with a superconducting quantum interference device (SQUID) amplifier (see below), as well as the verification of the above predictions for the noise, is a topic for future research.

Other quantum-limited, solid-state r.f. amplifiers

According to the above analysis, the SET approaches but does not quite reach the quantum limit. The back-action noise due to the

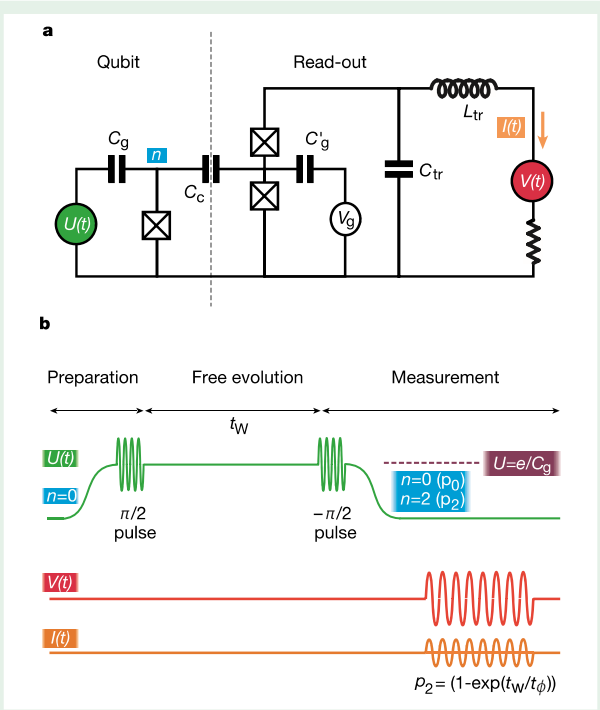

Figure 8 Measuring the state of a quantum system. **a**, Schematic circuit showing how a qubit implemented by a Cooper-pair box could be read-out by an r.f.-SET. **b**, Time evolution of signals in the circuit of **a**. While the read-out r.f.-SET is turned off, a first pulse prepares the qubit in a quantum superposition of ground and excited state at the crossing point $C_gU = e$. After a waiting period, a second pulse is applied which, in absence of decoherence, would make the qubit return to the ground state. Finally, after these manipulations, the read-out transistor is switched on while the box gate charge is moved away from $C_gU = e$. If decoherence occurs, the qubit will be left in the $n = 2$ charge state with a non-zero probability p_2. Given its sensitivity and low back-action noise, the r.f.-SET should be able to detect this event with a signal-to-noise ratio better than unity. C_{tr} and L_{tr} refer respectively to the capacitance and inductance of the impedance transformer. The times t_W and t_ϕ are the waiting time between the two pulses and the intrinsic decoherence time of the box, respectively.

randomness of tunnel events is dominated by phase-scrambling processes inside the island. But in the co-tunnelling regime, back-action noise is dominated by fluctuations of the island voltage associated with the measurement of the gate voltage itself and should therefore be more efficient. More work, experimental and theoretical, is needed to quantify this conjecture.

The superconducting SET can measure the charge on the gate with fully coherent carriers, the Cooper pairs. Zorin has analysed theoretically a version of this device shunted by a resistor and found that the noise energy could in this case exactly reach the quantum limit[29]. However, the mode of operation seems to involve a more precise tuning of the device parameters than for the SET.

So far we have considered voltage amplifiers, that is, amplifiers with an input impedance that is large compared with the resistance quantum R_K. For several years already, SQUID devices have played the role of the SET in the realm of low-impedance amplifiers. There is in fact a duality relationship between the d.c.-SQUID and the SET[1]. Whereas the SET is based on charge quantization of a metallic island surrounded by an insulator, the d.c.-SQUID is based on the quantization of flux in a superconducting loop. The sub-electron sensitivity of the SET has its analogue in the sub-flux quantum sensitivity of the SQUID. Although it has been known for many years that a SQUID could operate at the quantum limit, this has been achieved only recently in the r.f. domain. Andre *et al.* have shown that a SQUID with a microstrip input line could achieve $k_B T_N \simeq 5\hbar\omega$ at 438 MHz (ref. 30).

Finally, we should mention a special class of linear amplifiers: the mixers based on photon-assisted tunnelling in superconductor–insulator–superconductor (SIS) junctions. They convert a signal at several hundred GHz into a signal at several GHz. Even though the absolute power of the output signal is weaker than the power of the input signal, these devices have a large 'photon number' gain. Futhermore, their noise closely approaches the quantum limit: $E_N = 0.6\hbar\omega$ (ref. 31). Closely related to SIS mixers are Josephson parametric amplifiers, which have been operated at the quantum limit[32]. However, these devices do not have the advantage of the SET and the SQUID to amplify at the same time both a.f. and r.f. signals, a useful feature for tuning and trouble-shooting.

Measuring the state of a two-level system

In the past few years there has been much interest in the possibility of realizing a quantum computer[6]. Although the more advanced experiments in this field are taking place in quantum optics systems[33,34], several implementations of quantum bits and quantum gates in solid-state systems have been proposed[35–38]. We focus here on a charge qubit which is now well understood experimentally[12,13] and theoretically[39,40]: the Cooper-pair box (Fig. 7). It consists of a superconducting island with Coulomb energy E_C connected to a superconducting charge reservoir by means of a Josephson tunnel junction with Josephson coupling energy E_J. The island is influenced electrostatically through a gate capacitor C_g connected to voltage source (Fig. 7a). If the conditions $k_B T \ll E_J \ll E_C < \Delta$ are realized, where Δ is the energy gap of the superconductor, then the island will have only an even number n of excess electrons. This only degree of freedom will be a good quantum number, except at the avoided crossings of the charge levels (Fig. 7b,c). A recent experiment has shown that such a solid-state qubit was able to display several Rabi oscillations when stimulated by a microwave pulse[13]. However, the measurement scheme in this experiment involved a probe tunnel junction which observed the qubit continuously, but weakly. Such a continuous observation dephases the qubit and prevents a measurement of its intrinsic decoherence time. It is therefore desirable to read-out the qubit only at the end of the coherent manipulation and evolution period (Fig. 8). An obvious candidate for the read-out is the SET. In a version with r.f. bias[4], the transistor can be turned on and off very quickly, the turn-on time being set by the damping time of the tank circuit. This latter is of the order of several tens of nanoseconds, a time supposedly shorter than the intrinsic decoherence time of the box, estimated to be longer than 1 μs. The question therefore arises as to whether the SET is sufficiently sensitive to detect the state of the box with a signal-to-noise ratio allowing the study of decoherence mechanisms.

Measurement time and dephasing rate

An important concept is the measurement time T_m of the read-out SET[14], which is defined as the time needed for discriminating between the two charge states of the box differing by a Cooper pair, assumed to be good eigenstates, with a signal-to-noise ratio of 1. Island box charge is a good quantum number when $E_J/E_{el} \ll 1$, where the electrostatic energy $E_{el} = 2e^2(1 - C_gU/e)/C_{tot}$ of the box is controlled by the voltage U (here C_g and C_{tot} refer to the box gate capacitance and total island capacitance). In practice, the charge measurement is made just after U is varied away from the crossing point (Fig. 8b). The circuit of Fig. 8a shows that T_m is closely related to the voltage noise of the SET, with $T_m = 4S_V/(2e/C_{tot})^2$. We thus find that $T_m = (\delta Q/e)^2(C_{tot}/C_{in})^2$, where C_{in}/C_{tot} is the charge-coupling coefficient.

It is interesting to note that the back-action current noise dephases the charge states relative to one another only if charge is a

good quantum number. The general expression for the dephasing rate is

$$\Gamma_\phi = \left(\frac{e}{\hbar}\right)^2 \frac{E_{el}^2}{E_J^2+E_{el}^2} S_V^{box}(\omega=0)$$

where $S_V^{box}(\omega) = S_I(\omega)/C_{tot}\omega)^2$ is the fluctuation spectral density of the box island voltage induced by the SET current noise. In the regime $E_J/E_{el} \ll 1$, we find that the product $T_m\Gamma_\phi = 2[E_N(\omega)/\hbar\omega]^2_{\omega=0}$ involves only the noise energy and is of order unity. Once again, this is another close approach to the quantum limit as the minimum value for $T_m\Gamma_\phi$ is $\frac{1}{2}$ (Table 1).

So in principle it seems that the SET could acquire charge with any given large signal-to-noise ratio by measuring the box for a long enough time. However, any coupling between charge states will induce transitions and will corrupt the measurement. The transition rate between charge states due to the current noise is given by

$$\Gamma_1 = \left(\frac{e}{\hbar}\right)^2 \frac{E_J^2}{E_J^2+E_{el}^2} S_V^{box}(\omega=\Omega)$$

where $\Omega = \sqrt{E_J^2+E_{el}^2}/\hbar$ is the transition frequency between charge states.

We thus find that the signal-to-noise ratio including the effect of transitions between charge states is

$$S/N = (\Gamma_1 T_m)^{-1/2} = \frac{1}{(E_N/\hbar\omega)_{\omega=0}} \left(\frac{2E_J^2}{E_J^2+E_{el}^2}\right)^{-1/2}$$

In practice, a signal-to-noise ratio significantly greater than 1 seems possible with an optimized r.f.-SET in a single charge measurement, even when taking into account the 50% reduction in sensitivity of the SET in the r.f.-bias mode[41].

Towards single-photon sensitivity in the r.f. domain

To summarize, the SET transistor is a charge amplifying device whose sensitivity in the r.f. domain is limited in principle only by a well understood process, quantum shot noise. This property displays a marked contrast with a FET. It should be possible in the near future to show experimentally that the noise energy of the SET approaches the quantum limit within a factor of order unity. Although the SET will not be 100% efficient in acquiring charge information with only the minimal back-action noise required by quantum mechanics, it should still be able to read-out a charge qubit in a single-shot measurement. In more sophisticated devices using Cooper-pair tunnelling or co-tunnelling processes, the quantum limit could be approached even more closely. Furthermore, by transposing in the r.f. domain the manipulations of the quantum signal that are now performed routinely in experiments in cavity quantum electrodynamics[42], one could use these ultimate amplifiers for measuring signals consisting of a single photon, without even destroying the photon. □

1. Averin, D. V. & Likharev, K. K. Coulomb blockade of tunneling and coherent oscillations in small tunnel junctions. *J. Low Temp. Phys.* **62,** 345–372 (1986).
2. Fulton, T. A. & Dolan, G. J. Observation of single-electron charging effects in small tunnel junctions. *Phys. Rev. Lett.* **59,** 109–112 (1987).
3. Meirav U., Kastner, M. A. & Wind, S. J. Single-electron charging and periodic conductance resonances in GaAs nanostructures. *Phys. Rev. Lett.* **65,** 771–774 (1990).
4. Schoelkopf, R. J., Wahlgren, P., Kozhevnikov, A. A., Delsing, P. & Prober, D. The radio-frequency single-electron transistor (RF-SET): a fast and ultrasensitive electrometer. *Science* **280,** 1238–1242 (1998).
5. Mather, J. C. Super photon counters. *Nature* **401,** 654–655 (1999).
6. Steane, A. Quantum computation. *Rep. Prog. Phys.* **61,** 117 (1998).
7. Korotkov, A. N., Averin, D., Likharev, K. K. & Vasenko, S. A. in *Single-Electron Tunneling and Mesoscopic Physics* (eds Koch, H. & Lubbig, H.) 45–59 (Springer, Berlin, 1992).
8. Mar, D. J., Westervelt R. & Hopkins, P. F. Cryogenic field-effect transistor with single electronic charge sensitivity. *Appl. Phys. Lett.* **64,** 631–633 (1994).
9. Keller, M. W., Eichenberger, A., Martinis, J. M. & Zimmerman, N. M. A capacitance standard based on counting electrons. *Science* **285,** 1706–1709 (1999).
10. Schoelkopf, R. J., Moseley, S. H., Stahle, C. M., Wahlgreen, P. & Delsing, P. A concept for a submillimeter-wave single-photon counter? *IEEE Trans. Appl. Supercond.* **9,** 2935–2938 (1999).
11. Komiyama, S., Astafiev, O., Antonov, V., Kutsuwa, T. & Hirai, H. A single-photon detector in the far-infrared range. *Nature* **403,** 405–407 (2000).
12. Bouchiat, V., Vion, D., Joyez, P., Esteve, D. & Devoret, M. H. Quantum coherence with a single Cooper pair. *Phys. Scr.* **T76,** 165–170 (1998).
13. Nakamura, Y., Pashkin, Yu. A. & Tsai, J. S. Coherent control of macroscopic quantum states in a single-Cooper-pair box. *Nature* **398,** 786–788 (1999).
14. Shnirman, A. & Schoen, G. Quantum measurements performed with a single-electron transistor. *Phys. Rev. B* **57,** 15400–15407 (1997).
15. Naveh, Y. & Likharev, K. K. Modeling of 10-nm-scale ballistic MOSFET's. *IEEE Electron Devices Lett.* **21,** 242–244 (2000).
16. Devoret, M. H. & Grabert, H. in *Single Charge Tunneling* (eds Grabert, H. & Devoret, M. H.) 1–19 (Plenum, New York, 1992).
17. Grabert, H. Charge fluctuations in the single-electron box: perturbation expansion in the tunneling conductance. *Phys. Rev.* **50,** 17364–17377 (1994).
18. Schoeller, H. & Schoen, G. Mesoscopic quantum transport: resonant tunneling in the presence of a strong Coulomb interaction. *Phys. Rev. B* **50,** 18436–18442 (1994).
19. Shirakashi, J., Matsumoto, K., Miura, N. & Konagai, N. Single-electron charging effects in Nb/Nb oxide-based single-electron transistors at room temperature. *Appl. Phys. Lett.* **72,** 1893–1895 (1998).
20. Zhuang, L., Guo, L. & Chou, S. Y. Silicon single-electron quantum-dot transistor switch operating at room temperature. *Appl. Phys. Lett.* **72,** 1205–1207 (1998).
21. Pashkin, Yu. A., Nakamura, Y. & Tsai, J. S. Room-temperature Al single-electron transistor made by electron-beam lithography. *Appl. Phys. Lett.* **76,** 2256–2258 (2000).
22. Wolf, H. *et al.* Investigation of the offset charge noise in single electron tunneling devices. *IEEE Trans. Instrum. Measurement* **46,** 303–306 (1997).
23. Caves, C. M., Thorne, K. S., Drever, W. P., Sandberg, V. D. & Zimmermann, N. On the measurement of a weak classical force coupled to a quantum-mechanical oscillator. I. Issues of principle. *Rev. Mod. Phys.* **52,** 341–392 (1980).
24. Caves, C. M. Quantum limits on noise in linear amplifiers. *Phys. Rev. D* **26,** 1817–1839 (1982).
25. Braginsky, V. B. & Khalili, F. Ya. *Quantum Measurement* (Cambridge Univ. Press, 1992).
26. Pospieszalski, M. W. & Wollack, E. J. in *Proceedings of 2nd ESA Workshop on Millimetre Wave Technology and Applications(WPP-149)* 221–226 (ESA, Paris, 1998).
27. Gurvitz, S. A. Measurements with a noninvasive detector and dephasing mechanism. *Phys. Rev. B* **56,** 15215–15223 (1997).
28. Korotkov, A. N. Preprint cond-mat/0003225 at <http://xxx.lanl.gov> (2000).
29. Zorin, A. B. Quantum-limited electrometer based on single Cooper pair tunneling. *Phys. Rev. Lett.* **76,** 4408–4411 (1996).
30. André, M.-O., Mück, M., Clarke, J., Gail, J. & Heiden, C. Radio-frequency amplifier with tenth-kelvin noise temperature based on microstrip direct current superconducting quantum interference device. *Appl. Phys. Lett.* **75,** 698–700 (1999).
31. Mears, C. A. *et al.* Quantum-limited heterodyne detection of millimeter waves using superconducting tantalum tunnel junctions. *Appl. Phys. Lett.* **57,** 2487–2489 (1990).
32. Movshovich, R. *et al.* Observation of zero-point noise squeezing via a Josephson parametric amplifier. *Phys. Rev. Lett.* **65,** 1419–1422 (1990).
33. Turchette, Q. A., Hood, C. J., Lange, W., Mabuchi, H. & Kimble, H. J. Measurement of conditional phase shifts for quantum logic. *Phys. Rev. Lett.* **75,** 4710–4713 (1995).
34. Monroe, C. *et al.* Resolved-sideband Raman cooling of a bound atom to the 3D zero-point energy. *Phys. Rev. Lett.* **75,** 4011–4014 (1995).
35. Bocko, M. F., Herr, A. M. & Feldman, M. F. Prospects for quantum coherent computation using superconducting electronics. *IEEE Trans. Appl. Supercond.* **7,** 3638–3641 (1997).
36. Kane, B. E. A silicon-based nuclear spin quantum computer. *Nature* **393,** 133–137 (1998).
37. Loss, D. & DiVincenzo, D. P. Quantum computation with quantum dots. *Phys. Rev. A* **57,** 120–126 (1998).
38. Mooij, J. E. *et al.* Josephson persistent-current qubit. *Science* **285,** 1036–1039 (1999).
39. Averin, D. V. Adiabatic quantum computation with Cooper pairs. *Solid State Commun.* **105,** 657–659 (1998).
40. Makhlin, Yu., Schoen, G. & Shnirman, A. Josephson-junction qubits with controlled couplings. *Nature* **398,** 786–789 (1999).
41. Korotkov, A. N. & Paalanen, M. A. Charge sensitivity of radio frequency single-electron transistor. *Appl. Phys. Lett.* **74,** 4052–4054 (1999).
42. Nogues, C. *et al.* Seeing a single photon without destroying it. *Nature* **400,** 239–242 (1999).

Acknowledgements

This work was supported in part by the National Security Agency (NSA), the Advanced Research and Development Activity (ARDA) and the Army Research Office (ARO). One of us (M.H.D) acknowledges support from Commissariat à l'Energie Atomique (CEA). We thank D. Averin, J. Clarke, P. Delsing, D. Esteve A. Korotkov, K. Likharev, H. Mooij, D. Prober, G. Schoen and E. Wollack for helpful discussions and communications of results prior to publication.